HHS Public Access

Author manuscript

Free Radic Biol Med. Author manuscript; available in PMC 2017 July 01.

Published in final edited form as:

Free Radic Biol Med. 2016 July ; 96: 22–33. doi:10.1016/j.freeradbiomed.2016.04.002.

Reactive Oxygen Species Production in Cardiac Mitochondria After Complex I Inhibition: Modulation by Substrate-Dependent Regulation of the NADH/NAD$^+$ Ratio

Paavo Korge[a], **Guillaume Calmettes**[a], and **James N. Weiss**[a,b,*]

[a]UCLA Cardiovascular Research Laboratory and the Department of Medicine (Cardiology), David Geffen School of Medicine at UCLA, Los Angeles, California 90095

[b]Department of Medicine Physiology, David Geffen School of Medicine at UCLA, Los Angeles, California 90095

Abstract

Reactive oxygen species (ROS) production by isolated complex I is steeply dependent on the NADH/NAD$^+$ ratio. We used alamethicin-permeabilized mitochondria to study the substrate-dependence of matrix NADH and ROS production when complex I is inhibited by piericidin or rotenone. When complex I was inhibited in the presence of malate/glutamate, membrane permeabilization accelerated O_2 consumption and ROS production due to a rapid increase in NADH generation that was not limited by matrix NAD(H) efflux. In the presence of inhibitor, both malate and glutamate were required to generate a high enough NADH/NAD$^+$ ratio to support ROS production through the coordinated activity of malate dehydrogenase (MDH) and aspartate aminotransferase (AST). With malate and glutamate present, the rate of ROS production was closely related to local NADH generation, whereas in the absence of substrates, ROS production was accelerated by increase in added [NADH]. With malate alone, oxaloacetate accumulation limited NADH production by MDH unless glutamate was also added to promote oxaloacetate removal via AST. α-ketoglutarate (KG) as well as AST inhibition also reversed NADH generation and inhibited ROS production. If malate and glutamate were provided before rather than after piericidin or rotenone, ROS generation was markedly reduced due to time-dependent efflux of CoA. CoA depletion decreased KG oxidation by α-ketoglutarate dehydrogenase (KGDH), such that the resulting increase in [KG] inhibited oxaloacetate removal by AST and NADH generation by MDH. These findings were largely obscured in intact mitochondria due to robust H_2O_2 scavenging and limited ability to control substrate concentrations in the matrix. We conclude that in mitochondria with inhibited complex I, malate/glutamate-stimulated ROS generation depends strongly on oxaloacetate removal and on the ability of KGDH to oxidize KG generated by AST.

*Correspondence should be addressed: Department of Medicine (Cardiology), David Geffen School of Medicine at the University of California Los Angeles, Los Angeles, CA, 90095. Tel.: +310 825 9029; fax: +310 206 5777. jweiss@mednet.ucla.edu.

Keywords

Mitochondria; NADH generation/oxidation; complex I inhibition; ROS production

Introduction

Isolated mitochondria energized with physiologically relevant NAD^+-related substrates produce very little reactive oxygen species (ROS) as long as the NADH generated by the tricarboxylic acid (TCA) cycle is rapidly oxidized to maintain a low NADH/NAD^+ ratio. Consensus exists that for electron transport in the forward direction, ROS production by isolated complex I depends on the degree of flavin mononucleotide (FMN) reduction, the latter increasing with an elevated NADH/NAD^+ ratio, indicating a close relationship between ROS production and the redox potential of the NADH/NAD^+ couple [1–3]. Fully reduced flavin is an electron donor capable reducing O_2 at its substrate binding site. Indeed, in the absence of any other electron acceptors except O_2, NADH oxidation by purified complex I results in superoxide production that at [NADH]>1 μM becomes directly proportional to concentrations of complex I and O_2. An increase in [NAD^+] that lowers the NADH/NAD^+ ratio strongly inhibits ROS production. Because only the nucleotide-free binding site of reduced flavin is able to react with O_2, ROS production also depends on nucleotide concentrations as well as the NADH/NAD^+ ratio. Importantly, ROS production by isolated complex I does not require addition of ubiquinone pocket inhibitors like piericidin or rotenone, unless an electron acceptor to stimulate NADH consumption and generate NAD^+ is present [2, 4]. Because ubiquinone is extremely hydrophobic, amphiphilic ubiquinone analogs have been used as electron acceptors for isolated complex I, but they facilitate unphysiological side reactions that do not occur with endogenous ubiquinone [5].

Although rotenone- or piericidin-induced ROS production by cardiac mitochondria energized with NAD^+-related substrates is known to require high matrix NADH/NAD^+ ratio [6], experiments with intact mitochondria have certain limitations that make it difficult to study substrate-dependent regulation of NADH and ROS production. These limitations include rapid ROS scavenging in the matrix, low dicarboxylate carrier activity in cardiac mitochondria [7], decrease in matrix [KG] and [aspartate] in response to malate and glutamate addition and dependence of glutamate uptake on membrane potential [8, 9]. Given these factors, it is not surprising that rotenone addition to cardiac mitochondria energized with NAD-related substrates typically results in a relatively small increase in NADH fluorescence and ROS production [10, 11]. It remains still unclear why ROS production by complex I-inhibited mitochondria energized with NAD^+-related substrates is so variable and relatively low, generally reaching about 5–10% of that induced by succinate-supported reverse electron transport (for review see [12]). A reasonable assumption could be that low values and variability in ROS production are connected with substrate-dependent variations in NADH generation. However, for reasons presented above controlled manipulation of matrix [substrates] in intact mitochondria is very difficult if not impossible.

One way to study the importance of substrates in the regulation of NADH-supported H_2O_2 production in mitochondria with inhibited complex I is to use alamethicin-treated

mitochondria. Inner membrane permeabilization with alamethicin allows the matrix NADH/NAD^+ ratio to be rapidly manipulated by exogenous pyridine nucleotides, and has been previously used to demonstrated a close dependence of cardiac mitochondrial H_2O_2 production on the NADH/NAD^+ ratio [13]. In this study, we used this technique to explore the substrate-dependence of matrix NADH and ROS production when complex I is inhibited by piericidin or rotenone. Specifically, we tested the hypothesis that the NADH/NAD^+ ratio, and hence ROS production by mitochondria with inhibited Complex I in the presence of malate and glutamate, is regulated via the coordinated activity of malate dehydrogenase (MDH) and aspartate aminotransferase (AST), and that α-ketoglutarate (KG), either added or generated by AST, adds more complexity to this regulation. These findings may be relevant to ROS generation under pathophysiological conditions in which Complex I is inhibited or damaged, such as ischemia/reperfusion.

Material and Methods

Experimental techniques

This study was approved by the UCLA Chancellor's Animal Research Committee (ARC 2003-063-23B) and performed in accordance with the Guide for the Care and Use of Laboratory Animals published by the United States National Institutes of Health (NIH Publication No. 85-23, revised 1996) and with UCLA Policy 990 on the Use of Laboratory Animal Subjects in Research (revised 2010).

All measurements were carried out using customized Fiber Optic Spectrofluorometer (Ocean Optics) in a partially open continuously stirred cuvette at room temperature (22 to 24°C) [14]. Mitochondria were isolated from rabbit hearts as described previously [15]. Intact mitochondria were added (0.3 to 0.6 mg/ml) to incubation buffer containing 250 mM sucrose, 10 mM Hepes, pH 7.4 with Tris. Mitochondria were permeabilized with addition of alamethicin (20 μg/ml). Alamethicin creates pores which allow equilibration of low-molecular weight components across the inner membrane, while high-molecular weight proteins are retained in the matrix and intermembrane space [16]. Electron microscopy of alamethicin-treated mitochondria reveals no major disruption of membranes [16] and a consensus exists that enzymes, including those involved in ROS production, remain fully functional and have enhanced access to exogenously-delivered substrates [13, 16–18]. Piericidin was obtained from Cayman Chemical Company (Sapphire Bioscience) and succinyl phosphonate from MedChem Express (MCE). All other chemicals, including enzymes, were obtained from Sigma-Aldrich (St. Louis, MO). Mitochondria were pretreated with 1-chloro-2,4-dintrobenzene (CDNB) exactly as described previously [11].

H_2O_2 release from mitochondria was measured using 5 μM Amplex Red and 0.2 U Horse Radish Peroxidase (HRP) in the buffer (excitation/emission, 540/590 nm). The increase in resorufin fluorescence was calibrated by adding H_2O_2 in known concentrations.

Mitochondrial O_2 consumption was measured continuously by monitoring buffer O_2 content using a fiber optic oxygen sensor FOXY-AL300 (Ocean Optics) [14]

NADH fluorescence was recorded at 366/460 nm excitation/emission wavelengths and signal calibrated by adding NADH in known concentrations. In experiments where NAD^+ or NADH were added to permeabilized mitochondria to enhance the fluorescence signal or stimulate H_2O_2 production, NAD(H) concentration was chosen based on reports that H_2O_2 production by rotenone-inhibited permeabilized cardiac mitochondria exhibits a non-hyperbolic dependency on [NADH], with production close to maximum at about 100 μM, and decreasing at >200 μM [13].

Statistical analysis

For each data set, the mean and accompanying 95% confidence intervals (CIs) are reported. The conventional percentile bootstrap-resampling approach with 10,000 replications was used for estimating 95% CI as well as examining the significant difference between groups (effect size statistics) [19–21]. A P value <0.05 was considered statistically significant. All analyses were performed by subroutines for bootstrapping developed in the Python programming language [21].

Results

NADH production/oxidation by the coupled MDH and AST reactions regulates ROS production when complex I is inhibited

When mitochondria are exposed to piericidin or rotenone, ROS production by inhibited complex I or matrix dehydrogenases depends on the ability of the mitochondria to elevate the NADH/NAD^+ ratio [6]. Because the level of endogenous NAD(H) was too low to give a robust fluorescence signal, we added exogenous NAD^+ to Complex I-inhibited mitochondria to assess NADH generation after substrates were added. Using piericidin to inhibit complex I in alamethicin-permeabilized mitochondria, 5 mM malate caused only a small increase in NADH (Fig. 1A, blue trace), consistent with rapid inhibition of the MDH reaction due to oxaloacetate accumulation (Fig. 1D). Addition of 5 mM glutamate to remove oxaloacetate via the forward AST reaction led to a rapid and sustained increase in NADH, which was then rapidly oxidized by adding KG and aspartate to reverse the directions of the coupled AST and MDH reactions as indicated in Fig. 1D. Fig. 1B shows that H_2O_2 production under these conditions paralleled NADH production. Malate alone failed to significantly increase H_2O_2 production until glutamate was also added (blue trace). Moreover, when oxaloacetate removal by AST was inhibited by the AST inhibitor aminooxyacetate (AOA), glutamate no longer accelerated NADH generation or ROS production in the presence of malate (Fig. 1A and B, red traces). Under these conditions, however, ROS production could be increased significantly by addition of coenzyme A (CoA) and KG to facilitate NADH production by KGDH (see Fig. 1D).

Similar to malate alone, glutamate by itself also failed to significantly increase H_2O_2 production (Fig. 1B, green trace), which can be attributed to the relatively low glutamate dehydrogenase activity in cardiac mitochondria [22, 23]. Addition of malate, however, increased H_2O_2 robustly through the coupled activity of MDH and AST. The failure of malate alone to induce significant NADH production under our experimental conditions can be attributed to the lack of exogenously-supplied Mn^{2+} or Mg^{2+} in the buffer (see

supplemental information, Fig. S1), which is required by NAD^+-dependent malic enzyme to reduce NAD^+ [24] (see Discussion).

CoA, a key cofactor for KG oxidation by α-ketoglutarate dehydrogenase (KGDH), is expected to become depleted through alamethicin pores in permeabilized mitochondria. Addition of exogenous CoA during malate/glutamate-stimulated H_2O_2 generation had no significant effect (Fig. 1B, blue trace), indicating that the KGDH reaction (Fig. 1D) was not a major source of ROS under these conditions. However, in AST-inhibited mitochondria ROS production could be increased significantly by addition of CoA and KG to facilitate NADH production by KGDH (see Fig. 1D). This is illustrated in Fig. 1A (red trace), in which NADH generation by malate and glutamate was inhibited by AOA in piericidin-inhibited mitochondria, but rapidly and significantly activated after addition of both CoA and KG. Similarly, AOA addition was required to activate NADH generation after reversal of the AST reaction with KG and Asp to induce NADH oxidation. In the absence of AOA, addition of CoA and KG had no major effect on NADH production due to ability of the coupled MDH/AST reactions to maintain a low [NADH], as demonstrated by rapid increase in NAD^+ reduction after AOA addition (Fig. 1A, blue trace). These changes in NADH production also explain activation of H_2O_2 production after CoA and KG addition in AOA-inhibited mitochondria (Fig.1B, red trace). Fig. 1E summarizes H_2O_2 production by piericidin-inhibited mitochondria depending on glutamate and malate addition alone or together in the absence or presence of AOA (AST inhibitor), CoA and KG.

These findings demonstrate that the MDH and AST reactions are both readily reversible and can promote either NAD(H) reduction or oxidation depending on the concentration of substrates available to permeabilized mitochondria. The same properties were observed using purified MDH and AST (Fig. 1C). When malate was added to a suspension of NAD, MDH and AST, NADH fluorescence increased rapidly but modestly and quickly plateaued (blue trace), indicating that the MDH reaction had achieved equilibrium between forward and reverse directions due to accumulation of oxaloacetate and NADH. Addition of glutamate led to a robust further increase in NADH fluorescence reflecting the contribution of the AST reaction to NADH production (blue trace). However, if KG and Asp, the end-products of the AST reaction were added, NADH fluorescence returned to its baseline prior to addition of malate, indicating complete NADH conversion to NAD^+ by the combined MDH and AST reactions in the reverse direction. Alternatively, if AOA was added to the suspension to inhibit AST, malate caused the same initial increase in NADH fluorescence, but subsequent addition of glutamate caused no further increase (red trace).

The importance of functional coupling between MDH and AST for ROS production can be demonstrated also in intact cardiac mitochondria. Fig. 2 shows that malate addition to piericidin-inhibited intact mitochondria had little effect on H_2O_2 production that modestly increased after glutamate addition. Note that permeabilization resulted in a further significant increase in H_2O_2 production (Fig. 2, blue trace). In AOA-inhibited mitochondria, on the other hand, glutamate only slightly increased H_2O_2 production and alamethicin addition had no further significant effect (Fig. 2, red trace). The bar graph shows average rates for malate- and glutamate-stimulated ROS production in the absence or presence of AOA, recorded before and after inner membrane permeabilization. In general, these results

suggest that H_2O_2 production can be down-regulated by AST inhibition, but the effect of this inhibition is better expressed in permeabilized mitochondria.

The reversibility of the coupled MDH and AST reactions in regulating NADH and H_2O_2 production when complex I is inhibited is further illustrated in Fig. 3A. When permeabilized mitochondria were exposed to piericidin, H_2O_2 production induced by 1 mM malate and glutamate was suppressed by adding 0.1 mM KG and Asp to promote reversal of the coupled MDH/AST reactions, either before (red trace) or after (blue trace) addition of malate and glutamate. Further increasing the malate and glutamate concentrations (to 6 mM each) to promote the MDH reaction in the forward direction then increased ROS production. Bar graph in Fig. 3A shows average rates for malate/glutamate induced H_2O_2 production, KG/Asp-induced inhibition and reactivation of H_2O_2 production by higher malate/glutamate concentration.

The effects of KG and Asp in Fig. 3A deserve further comment. In intact mitochondria, KG would normally be metabolized by KGDH, which is also capable of generating ROS in the presence of a high NADH/NAD^+ ratio [25, 26]. However, the observation that KG suppressed, rather than increased ROS production in permeabilized mitochondria in Fig. 3A indicates that any contribution of KGDH to increased ROS production was offset by KG's reversal of the AST and MDH reactions promoting NADH oxidation under those conditions. As indicated in Fig. 1D, the ability of KGDH to oxidize KG depends on the availability of CoA as a required co-factor. In permeabilized mitochondria, however, CoA is depleted through alamethicin pores, which consequently limits KG oxidation. Fig. 3B shows that when permeabilized mitochondria (in the absence of complex I inhibitors and NAD^+ as an electron acceptor) were provided with KG as their sole substrate, addition of CoA to facilitate KG oxidation by KGDH increased ROS production, albeit to a significantly lesser extent (3.7 times) than addition of malate and glutamate in piericidin-inhibited mitochondria (Fig. 1B and 3A). Addition of the KGDH inhibitor succinyl phosphonate (SP,2 mM; Fig. 3B) under these conditions suppressed ROS production, confirming their origin from KGDH. SP is a KG analog that targets the KG binding component of KGDH to inhibit activity [27].

Inner membrane permeabilization significantly accelerates malate/glutamate oxidation and piericidin-dependent ROS production

Fig. 3C shows that O_2 consumption by malate/glutamate energized mitochondria is significantly increased after alamethicin addition, which dissipates membrane potential and also enhances substrate access to matrix enzymes. On average membrane permeabilization increased O_2 consumption three-fold (Fig. 3C, bar graph) and a higher rate was maintained for at least 4–5 min suggesting that NAD(H) efflux is a relatively slow process (see suppl. Fig. S2). However, in the experiment shown in Fig. 3C, NAD^+ was added to ensure that NAD(H) efflux did not limit electron transport and thereby modify the effect of KG on O_2 consumption. Under these conditions, KG addition rapidly inhibited O_2 consumption, most likely due to a decreased supply of NADH to complex I as a result of inhibition of NADH production by MDH (see Fig. 1D). Because complex I activity maintained a low NADH/NAD^+ ratio, CoA addition enhanced KG oxidation by KGDH (Fig. 3C). However,

note that an increase in [NADH], which inhibits KG oxidation by KGDH and favors reversal of MDH especially at high [KG], also inhibits the effect of CoA on H_2O_2 production by KGDH (Fig. 1B&3D). The increase in O_2 consumption after CoA addition was inhibited with SP suggesting that NADH was mainly generated by KGDH. The average increase in O_2 consumption after adding alamethicin to malate/glutamate-energized mitochondria and inhibition with KG is summarized in the bar graph of Fig. 3C.

In Fig. 3D, piericidin was added to intact mitochondria followed by malate and glutamate, which increased H_2O_2 production. The relatively low rate of ROS production by intact mitochondria was rapidly and drastically increased by alamethicin and decreased by KG addition. Subsequent addition of CoA had little effect, but inhibition of AST increased H_2O_2 production. These results are consistent with those in Fig.1 and indicate that KG can drive AST in reverse direction, resulting in oxaloacetate accumulation and NADH oxidation by MDH that explains inhibition of ROS production with KG addition. Under those conditions inhibition of NADH oxidation by MDH, secondary to inhibition of AST, allows NADH generation by KGDH to increase (after addition of KG and CoA) to the level required for ROS production by KGDH and any other flavin-dependent enzymes known to produce ROS at high NADH/NAD^+ ratios. The average H_2O_2 production by piericidin-inhibited intact mitochondria after malate/glutamate addition, acceleration of H_2O_2 production after alamethicin, inhibition by KG and acceleration after CoA and AOA addition is shown in the bar graph of Fig. 3D.

Note that alamethicin addition to malate/pyruvate-energized mitochondria failed to increase O_2 consumption and stimulate H_2O_2 production relative to piericidin-inhibited intact mitochondria (see suppl. Fig. S2). A simple explanation is that generation of Acetyl-CoA, required for oxaloacetate removal under those conditions, depends on CoA availability and CoA efflux starts limiting Acetyl-CoA/NADH production by pyruvate dehydrogenase (PDH) despite presence of pyruvate. These results also suggest that CoA efflux via alamethicin pores is much faster compared to NAD(H) efflux.

The importance of NADH generation versus the concentration of added NADH

Like CoA, pyridine nucleotides are small enough to diffuse through alamethicin pores. However, prior evidence indicates that a significant NAD(H) fraction remains bound to matrix proteins [28, 29] which is only very slowly depleted below the level required for reduction of proteins responsible for ROS production. To determine how the total available pool of NAD(H) influences ROS production, we added graduated doses of NADH to piericidin-inhibited permeabilized mitochondria in the absence of malate and glutamate (Fig. 4). NADH addition stimulated H_2O_2 production in a dose-dependent manner that gradually slowed as NADH was oxidized. However, in each case, addition of malate and glutamate boosted H_2O_2 production to nearly identical rates, despite large differences in the total added NADH pools (from 0 to 100 μM). The inset in Fig. 4 (upper left corner) shows that after adding NADH to piericidin-inhibited permeabilized mitochondria, NADH fluorescence slowly declined, but addition of malate and glutamate reversed this decline. Thus, loss of endogenous matrix NAD(H) through the alamethicin pores had little effect of H_2O_2

production rates over the time course studied as long as the NADH/NAD^+ ratio in the vicinity of ROS producing site(s) could be maintained at a high level.

Effects of the order of substrate-inhibitor addition on piericidin- or rotenone-stimulated ROS production in permeabilized mitochondria

An interesting phenomenon occurred when piericidin or rotenone were added to permeabilized mitochondria after, rather than before, malate and glutamate. When piericidin was added to permeabilized mitochondria before malate and glutamate, the increase in H_2O_2 production was rapid and robust (Fig. 5A, red trace). Surprisingly, however, if piericidin was added after substrates (traces b-e), ROS production rate progressively decreased as the time delay increased. Similar results were obtained with rotenone in place of piericidin (Fig. 5B). Fig. 5C and D summarize the results for piericidin or rotenone correspondingly, added either before or 2 min after malate/glutamate and antimycin or AA5 plus antimycin effects on H2O2 production in 4–6 mitochondrial preparations.

Fig. 6 shows NADH generation under the same experimental conditions as in Fig.5. To boost the NADH fluorescence signal, we added exogenous NAD^+ to piericidin or rotenone-inhibited mitochondria to assess NADH generation. Similar to the robust stimulation of ROS production when piericidin or rotenone were added before substrates (red traces in Fig. 5A and B), NADH production was also robust (red traces in Fig. 6A and B). However, when malate and glutamate were added before piericidin or rotenone, NADH production decreased progressively as the time delay increased (traces b-e in Fig. 6A and B). Note that addition of [KG] and [Asp] at the end of traces rapidly decreased NADH fluorescence by reversing the direction of MDH reaction towards NADH oxidation.

The relationship between NADH generation and H_2O_2 production from the data in Figs. 5 and 6 is plotted in Fig. 7. The steep relationship between NADH generation and H_2O_2 production by complex I-inhibited permeabilized mitochondria agrees with the experimental findings that ROS production by purified complex I or KGDH requires a high NADH/NAD^+ ratio [1, 2, 25, 26].

Why does the order of substrate/inhibitor addition have such a strong influence on NADH generation and H_2O_2 production? As shown above (Fig. 3C), KG oxidation by KGDH is inhibited due to CoA loss from the matrix in permeabilized mitochondria. In the absence of AOA and complex I inhibitors and in the presence of malate and glutamate, NADH and oxaloacetate generated by MDH are rapidly consumed by complex I and AST, resulting in KG and aspartate production. If, under these conditions, matrix CoA depletion decreases KG oxidation by KGDH, causing [KG] to increase and inhibit NADH generation by MDH (see Fig. 1D), this could explain why the subsequent addition of piericidin or rotenone to inhibit complex I resulted in reduced H_2O_2 production, compared to the case when the inhibitors were added before malate and glutamate (Fig. 5) and substrate accumulation. In this case, adding exogenous CoA to facilitate KG oxidation should accelerate H_2O_2 production. Fig. 8 shows that this is the case. Compared to robust H_2O_2 production when piericidin was added before malate and glutamate (blue trace), the slow rate of H_2O_2 production when malate and glutamate were added before piericidin accelerated after addition of CoA (purple trace), but did not reach the level in the blue trace. Apparently sufficiently high [KG] that is close to or

higher than the K_m of KGDH for KG (which in cardiac mitochondria is about 0.2 mM [30]) was generated by AST in a ternary complex to enhance KG oxidation and NADH production by KGDH. However, when AST was inhibited from the start of the incubation and therefore very little KG and NADH were present at the time of CoA addition, KG addition was required to increase H_2O_2 production, irrespective whether piericidin was added before or after substrates (green and red traces). The almost equal increase in H_2O_2 production also indicates that NAD(H) available for KGDH under those two conditions was not significantly different. Note that in the absence of CoA, H_2O_2 generation associated with the rapid increase in [NADH] in piericidin-inhibited mitochondria was effectively inhibited by KG (blue trace). Average rates of CoA/KG-induced H_2O_2 production relative to that stimulated with piericidin and malate/glutamate addition are shown in Fig. 8B.

Finally, although ROS production was markedly decreased as the time delay between the addition of substrates and piericidin or rotenone increased, antimycin was capable of rapidly accelerating ROS production under these conditions (Fig. 5A and B, green and orange traces). This increase involved ubiquinone reduction in complex II because atpenin A5 (AA5), a specific inhibitor of ubiquinone reduction, completely prevented the antimycin-induced ROS increase (Fig. 5A and B, orange and green traces), as did malonate (5 mM) added at the start of incubation (not shown). These results imply that at the time of antimycin addition, the matrix contained sufficient succinate to be oxidized for ubiquinol generation and ROS production by complex III. Succinate could either be generated via reversal of succinate dehydrogenase reaction (complex II) or from succinyl-CoA generated by KGDH. However, since inner membrane permeabilization is expected to increase CoA efflux and therefore inhibit KG oxidation and succinyl-CoA generation by KGDH [3, 25], the latter route seems unlikely under these conditions. This was confirmed by adding succinyl phosphonate (SP) to inhibit KGDH [3, 27], which had no suppressive effect on antimycin-induced ROS production (Fig. 5B, purple trace), indicating that succinate was either already present or mainly generated via reversal of the succinate dehydrogenase reaction before antimycin addition.

Factors masking ROS production by piericidin-inhibited intact mitochondria in the presence of malate/glutamate

In intact mitochondria, rotenone or piericidin have been shown to induce only modest ROS production in the presence of NAD^+-related substrates [31–38], as we confirmed in Fig. 2&3D. The effects that we have observed in permeabilized mitochondria are likely to be masked in intact mitochondria for several reasons. First, intact mitochondria have much greater matrix H_2O_2 scavenging capacity than permeabilized mitochondria, since in the latter case key antioxidants such as glutathione are depleted through alamethicin pores. In addition membrane potential dissipation eliminates also transhydrogenase activity that links substrate oxidation to H_2O_2 removal. This is illustrated in Fig. 9 in which intact (solid lines) versus permeabilized mitochondria (dashed lines) were exposed to piericidin, malate and glutamate to stimulate H_2O_2 production for a period of four minutes before Amplex Red/HRP was added to detect the accumulated H_2O_2 (indicated by the initial jump in fluorescence when Amplex Red/HRP was added). In permeabilized mitochondria, the piericidin-induced H_2O_2 accumulation was significant, especially when piericidin had been

added before (blue dashed line) rather than after malate and glutamate (red dashed line). In intact mitochondria, however, there was no detectable H_2O_2 accumulation under either condition (blue and red solid lines). Thus, in intact mitochondria, most of the H_2O_2 was effectively scavenged before it could leave the matrix to accumulate in the buffer.

Although alamethicin permeabilization results in a major decrease in antioxidant activity, the matrix still retains an active thioredoxin/peroxiredoxin system. To demonstrate that substrate-dependent activation of this system, possibly via NADPH generation by glutamate dehydrogenase, is not responsible for lower H_2O_2 production when oxidation of substrates was allowed before complex I inhibition, we used mitochondria treated with CDNB as described previously [11]. CDNB is effective inhibitor of thioredoxin reductase that is essential for the thioredoxin/peroxiredoxin system to operate. The results presented in the supplement (Fig. S3) show that H_2O_2 production by CDNB-treated mitochondria when complex I was inhibited before or after adding malate/glutamate was similar to that in Fig. 5A, i.e. when piericidin was added during accelerated malate/glutamate oxidation, it induced relatively low H_2O_2 production.

These results, together with substrate-dependent reversibility of NADH/H_2O_2 production in permeabilized mitochondria, suggest that the actual concentration of substrates/products in the vicinity of reversible matrix enzymes have an important role. Cardiac mitochondria reportedly exhibit dicarboxylate carrier activity that is six times lower compared with liver mitochondria [7]. In addition to relatively low carrier activity, glutamate uptake through glutamate/aspartate antiporter is electrogenic and requires membrane potential [8, 9]. Because complex I inhibition results in membrane potential dissipation, glutamate added after piericidin or rotenone may have limited access to the matrix to facilitate the coupled MDH/AST reaction as required for robust NADH and H_2O_2 production. Importantly, glutamate and malate transport into mitochondria requires aspartate and KG efflux. Together, these factors make it extremely difficult to adjust matrix substrate concentrations accurately as required to study the importance of functional coupling between MDH/AST and the role KG consumption in regulation of NADH and ROS generation using intact mitochondria.

Discussion

It is well-established that the basic mechanism of ROS production by isolated complex I involves FMN reduction by NADH and depends on high free NADH/NAD^+ ratio as well as on enzyme and O_2 concentrations, provided that there are no other electron acceptors present except O_2 [1, 2]. Assessing the mechanism of ROS production by complex I in isolated mitochondria in the presence of NAD^+-related substrates, however, is more complicated and must take into consideration multiple factors. These include the rate of NADH generation/oxidation in the matrix that is regulated by supply of substrates, accumulation of products, the degree of inhibition of NADH oxidation by complex I, and the scavenging of H_2O_2 before it leaves the matrix. In addition several matrix dehydrogenases, most importantly KGDH, could be involved in ROS production after complex I inhibition [3].

In this study we analyzed the importance of functional coupling between MDH and AST in malate/glutamate-induced NADH generation and ROS production in permeabilized mitochondria inhibited by piericidin or rotenone. As a model system to gain mechanistic insight into the role of MDH-AST coupling in NADH production and ROS generation, permeabilized mitochondria have several advantages: a) the concentration of all low molecular weight compounds in the matrix can be readily adjusted; b) decrease in antioxidant system activity in the matrix that allows more H_2O_2 to diffuse out of the matrix and be detected by Amplex Red/HRP.

Alamethicin-treated mitochondria have been frequently used to study enzymes that are retained in the matrix after permeabilization [16, 17] and also to allow measurement of NADH-induced ROS production, depending on NADH/NAD^+ ratio, since added nucleotides and substrates have direct access to the matrix and the matrix antioxidant capacity is reduced after permeabilization [13]. Although alamethicin-permeabilized mitochondria have been recommended as a preparation for quantifying the activities of NADH dehydrogenases and other enzymes under conditions that resemble their native environment [13, 16–18, 39, 40], we avoided the conventional approach in which mitochondria were first permeabilized with alamethicin, then alamethicin and the released low molecular weight metabolites were washed away, mitochondria stored on ice and used within next 3–4 hours. This technique may cause severe NAD(H) depletion during the incubation. Inner membrane permeabilization is expected to increase O_2 consumption as mitochondria work to recover $\Delta\Psi$ (Fig. 3C & S2A). In the presence of NAD^+-related substrates, pyridine nucleotide efflux through the pores starts limiting O_2 consumption while oxidation of matrix succinate is still stimulated. In our experiments, we measured mitochondrial ROS production within minutes after permeabilization and found that NAD(H) efflux through alamethicin-generated pores was not significant enough to affect malate/glutamate-induced H_2O_2 production in rotenone- or piericidin-inhibited mitochondria, at least during duration of experiments in this study. This is consistent with data from isolated porcine heart mitochondria in which time-resolved fluorescence spectroscopy revealed that >80% of NADH fluorescence was attributed to protein-bound NADH [28]. However, in the presence of substrates, NADH binding to proteins is transient. Assuming that: 1) significant fraction of bound NADH is associated with MDH [41] and complex I [29]; and 2) MDH binding to complex I favors direct coupling between NADH production and oxidation ([42–44] but see also [18]), it is possible that a high free NADH/NAD^+ ratio is generated close to flavin NADH binding sites. This can be accomplished by MDH working in the forward direction and with only limited amounts of pyridine nucleotides in the vicinity of NADH binding site, since in the absence of NAD, ROS production from purified complex I becomes independent of [NADH] at concentrations > 1 μM [2]. These arguments are consistent with the evidence presented in Fig. 4 showing that H_2O_2 production was closely related to malate/glutamate-stimulated mitochondrial NADH regeneration, irrespective of total matrix NADH content. In other words, the rate of ROS production was primarily regulated by the local NADH/NAD^+ ratio in the vicinity of ROS producing sites rather than bulk [NADH] in the matrix.

This study demonstrates that when complex I is inhibited by piericidin or rotenone, oxaloacetate accumulation due to lack of glutamate or accumulation of KG can limit or or reverse NADH production by the coupled MDH and AST reaction, thereby lowering the

NADH/NAD^+ ratio sufficiently to suppress ROS production in mitochondria with inhibited complex I. The unfavorable equilibrium of MDH reaction ([malate]/[oxaloacetate] $>10^4$) makes rapid removal of oxaloacetate a key requirement to avoid inhibition of NADH production or reversal of this reaction. It has been proposed that a transfer of oxaloacetate from MDH to AST is facilitated by structural organization that places these two enzymes in close proximity [45]. Malate-glutamate oxidation could be further enhanced by AST binding to KGDH [46]. Key role of KG in the regulation of ROS production under our experimental conditions seems to be related to KG generation within the ternary (MDH, AST, KGDH) complex. Direct transfer of substrates within this complex permits significantly higher reaction rates compared to free ligand diffusion [47]. These higher rates are most likely connected with higher local concentrations and specifically an increase in [KG] at AST binding site due to inhibited KG oxidation by KGDH. This could easily result in oxaloacetate accumulation and reverse MDH reaction under those conditions, especially when [NADH] is high and [malate] low. Unfortunately, as with many other enzymatic reactions proposed to sense local microenvironments, experimental evidence comes from functional studies [48, 49] because changes in global [metabolites] are expected to be small compared with local changes.

In connection with regulation of the MDH reaction, it is worth of mentioning that the isolated enzyme is inhibited in the forward direction by NADH, especially as malate concentration decreases [50]. An increased NADH/NAD^+ ratio also inhibits PDH and NADH generation by all regulatory enzymes of the TCA cycle. Malate/glutamate addition to isolated intact mitochondria results in a major increase in NADH fluorescence but almost no effect on ROS production, whereas subsequent addition of rotenone which induces a 6–10 times smaller increase in [NADH] is fully responsible for ROS production [10, 11]. Compared with rotenone-inhibited forward electron transport, succinate is known to induce higher matrix [NADH] levels and also much higher ROS production. Assuming that ROS production by complex I during forward or reverse electron transport has a unified mechanism that depends on flavin site reduction by NADH set by NADH/NAD^+ ratio [4], the above mentioned differences in ROS production could be explained by the NADH/NAD^+ ratio in the vicinity of flavin sites. It remains to be clarified whether or not the limited increase in NADH fluorescence induced by complex I inhibition in the presence of malate/glutamate is at least partially related to product inhibition of NADH production by the [NADH] increase. Inner membrane permeabilization may decrease product inhibition and also increase the concentration of reduced sites that are nucleotide free and can react with O_2 to form superoxide.

The difficulty in demonstrating how malate/glutamate/KG are involved in NADH/H_2O_2 production in intact mitochondria have been discussed above. In addition, isolated mitochondria are known to contain endogenous substrates, including glutamate in millimolar concentrations [51, 52]. This might explain why malate alone can stimulate H_2O_2 production after rotenone addition to intact mitochondria, albeit at a low rate [3]. Aspartate addition inhibited H_2O_2 production [3], probably because rotenone-induced dissipation of membrane potential is expected to stimulate aspartate uptake in exchange for matrix glutamate [53]. However, the aspartate effect was potentiated with ATP [3], which may generate some membrane potential in rotenone-inhibited mitochondria, and thereby enhance

aspartate efflux in exchange for glutamate. Because no extramitochondrial glutamate was present in these experiments and aspartate/glutamate exchange (1:1) did not occur, aspartate may indirectly inhibit KGDH by decreasing concentration of its substrates, KG and CoA as suggested previously [3].

Besides complex I, several flavin-dependent enzymes in the matrix are capable of producing ROS. Depending on the substrates present, ROS production by KGDH and PDH can be significantly higher than by complex I [3]. We have shown that KG and CoA addition to permeabilized mitochondria increases ROS production (Fig. 2B), although at a lower rate compared to that after addition of piericidin/malate/glutamate. Similar results have been published recently with permeabilized skeletal muscle mitochondria [3]. Additional experiments with intact mitochondria suggested that KGDH produces ROS at high rates mainly when oxidizing KG, whereas the reverse reaction from NADH seems to have less importance [3]. ROS is produced from the flavin of E3 component of KGDH that can be reduced by electrons generated due to KG oxidation in the forward reaction or by electrons from NADH in the reversed reaction. However, H_2O_2 production during KG oxidation by isolated KGDH is strongly stimulated by NADH and inhibited by NAD^+ addition, suggesting that NADH/NAD^+ ratio appears to be an important regulator [26]. In our experiments with piericidin or rotenone causing a high NADH/NAD^+ ratio, it is difficult to distinguish between NADH-induced ROS production from flavin sites of complex I and/or KGDH in the matrix in the absence of an available NADH binding site inhibitor specific for complex I or KGDH.

Because KG oxidation was most likely inhibited due to CoA efflux in permeabilized mitochondria, we assume that ROS production under our conditions was predominantly due to NADH generation and an increased NADH/NAD^+ ratio stimulating ROS generation by inhibited complex I and by possibly several other NAD(H)-linked flavin-containing matrix enzymes [3].

Different from the high NADH/NAD^+ ratio requirement for ROS production by complex I and other matrix NADH/NAD^+ isopotential flavoenzymes, maximal ROS production by complex III in the presence of succinate and antimycin requires partially oxidized ubiquinone pool [54]. The requirement for oxidized ubiquinone may indicate that electrons are donated to O_2 by reverse electron transfer from reduced heme B_L via ubiquinone [54]. This mechanism offers an explanation why a) complex II inhibition increases ROS production by antimycin-inhibited complex III in the presence of exogenous succinate [55] and b) stigmatellin-sensitive ROS production by antimycin-inhibited complex III has a bell-shaped response to succinate or malate/glutamate concentration. In this case, ROS production peaks at about 1 mM and then decreases with further increases in substrate concentration [56]. It also explains why oxidation of endogenous succinate was capable of inducing significant ROS production by antimycin-inhibited complex III (Fig. 5).

Finally we want to underline that we studied the regulation of NADH and ROS production during complex I inhibition in permeabilized mitochondria in the presence of glutamate and malate but in the absence of exogenous pyruvate. As we have shown malate/pyruvate-energized mitochondria respond to alamethicin differently because CoA efflux inhibits

NADH and Acetyl-CoA generation by PDH (Fig. S2). In intact mitochondria Acetyl-CoA generation by PDH is expected to decrease the rate of glutamate transamination as Acetyl-CoA competes for the available oxaloacetate [57]. However, if significant ROS are being produced, citrate oxidation may be inhibited because aconitase is highly sensitive to superoxide [58]. After significant inhibition of aconitase by superoxide or H_2O_2 [59], the TCA cycle segment from KG to oxaloacetate is still functional and can generate NADH, provided that KG, CoA and NAD^+ are available and KGDH is not significantly inhibited by ROS [59]. KGDH competition with pyruvate dehydrogenase for CoA has led to the suggestion that TCA operates in two segments: one from Acetyl-CoA to KG and second from KG to oxaloacetate [60]. In addition, cardiac mitochondria contain NAD^+-dependent malic enzyme that can oxidize malate and reduce NAD^+, producing pyruvate and CO_2 [24]. As shown in supplemental Fig. S1, this mechanism of NADH production was strictly Mg^{2+}- or Mn^{2+}-dependent and because pyruvate is generated in this reaction, NADH production was enhanced also by CoA addition to permeabilized mitochondria. CoA alone had no effect on malate-dependent NAD^+ reduction, which rapidly accelerated upon addition of $MgCl_2$ and then, was completely inhibited by Mg^{2+} chelation with EDTA. However, NADH production via MDH could be activated again by glutamate addition in the absence of free Mg^{2+} (Fig. S1). Mn^{2+} had similar effects as Mg^{2+}, with malic enzyme activation taking place at even lower [Mn^{2+}] than [Mg^{2+}]. CoA addition accelerated Mn^{2+}-dependent NADH production, especially at low concentrations of $MnCl_2$, indicating that CoA dependent pyruvate decarboxylation was involved. MgATP hydrolysis by F_1F_0 ATPase in response to $\Delta\Psi$ dissipation is expected to increase matrix free [Mg^{2+}] because ATP has a higher affinity for Mg^{2+} than ADP [61], but it is unclear whether or not this increase is enough to enhance malate-dependent NADH generation by malic enzyme. Whether malic enzyme is activated by changes in matrix [Mn^{2+}] is also unknown. Therefore, the conditions required for NADH generation by malate oxidation alone need further clarification. In our experiments with malate and glutamate, the lack of pyruvate excludes the role of the first segment, and therefore only the second segment coupled to the malate/aspartate shuttle can be analyzed. Nevertheless, the results presented in this study suggest that NADH/NAD^+-dependent ROS production by complex I, KGDH and possibly other matrix NAD/NADH consuming flavoproteins is closely regulated by changes in matrix [KG], underlining critical importance of KGDH complex activity in regulating the directionality of malate ↔ oxaloacetate step [60]. More generally, our findings highlight the complexity in dissecting the roles of various electron transport chain complexes and substrate/enzyme interactions in generating ROS under pathophysiological conditions such as ischemia/reperfusion.

Supplementary Material

Refer to Web version on PubMed Central for supplementary material.

Acknowledgments

This work was supported by NIH/NHLBI grants R01 HL101228, R01 HL117385, AHA Western States Affiliate Post-doctoral Research Fellowship 11POST6110007, and the Laubisch and Kawata Endowments. GC was supported by a Postdoctoral Fellowship award (No. 11POST6110007) from the American Heart Association, Western States Affiliate.

Abbreviations

Ala	alamethicin
AOA	aminooxyacetate
Ant	antimycin
AST	aspartate aminotransferase
Asp	aspartate
AA5	atpenin A5
CDNB	1-chloro-2,4-dintrobenzene
CoA	coenzyme A
FMN	flavin mononucleotide
Glu	glutamate
KG	α-ketoglutarate
KGDH	α-ketoglutarate dehydrogenase
Mal	malate
MDH	malate dehydrogenase
Mito	mitochondria
PDH	pyruvate dehydrogenase
Pier	piericidin
Rot	rotenone
SP	succinyl phosphonate

References

1. Hirst J, King MS, Pryde KR. The production of reactive oxygen species by complex I. Biochem Soc Trans. 2008; 36(Pt 5):976–980. [PubMed: 18793173]
2. Kussmaul L, Hirst J. The mechanism of superoxide production by NADH:ubiquinone oxidoreductase (complex I) from bovine heart mitochondria. Proc Natl Acad Sci U S A. 2006; 103(20):7607–7612. [PubMed: 16682634]
3. Quinlan CL, Goncalves RL, Hey-Mogensen M, Yadava N, Bunik VI, Brand MD. The 2-oxoacid dehydrogenase complexes in mitochondria can produce superoxide/hydrogen peroxide at much higher rates than complex I. J Biol Chem. 2014; 289(12):8312–8325. [PubMed: 24515115]
4. Pryde KR, Hirst J. Superoxide is produced by the reduced flavin in mitochondrial complex I: a single, unified mechanism that applies during both forward and reverse electron transfer. J Biol Chem. 2011; 286(20):18056–18065. [PubMed: 21393237]
5. Drose S, Brandt U. Molecular mechanisms of superoxide production by the mitochondrial respiratory chain. Adv Exp Med Biol. 2012; 748:145–169. [PubMed: 22729857]

6. Murphy MP. How mitochondria produce reactive oxygen species. Biochem J. 2009; 417(1):1–13. [PubMed: 19061483]
7. Saint-Macary M, Foucher B. Comparative partial purification of the active dicarboxylate transport system of rat liver, kidney and heart mitochondria. Biochem Biophys Res Commun. 1985; 133(2): 498–504. [PubMed: 4084286]
8. LaNoue KF, Tischler ME. Electrogenic characteristics of the mitochondrial glutamate-aspartate antiporter. J Biol Chem. 1974; 249(23):7522–7528. [PubMed: 4436323]
9. LaNoue KF, Bryla J, Bassett DJ. Energy-driven aspartate efflux from heart and liver mitochondria. J Biol Chem. 1974; 249(23):7514–7521. [PubMed: 4436322]
10. Kushnareva Y, Murphy AN, Andreyev A. Complex I-mediated reactive oxygen species generation: modulation by cytochrome c and NAD(P)+ oxidation-reduction state. Biochem J. 2002; 368(Pt 2): 545–553. [PubMed: 12180906]
11. Quinlan CL, Treberg JR, Perevoshchikova IV, Orr AL, Brand MD. Native rates of superoxide production from multiple sites in isolated mitochondria measured using endogenous reporters. Free Radic Biol Med. 2012; 53(9):1807–1817. [PubMed: 22940066]
12. Starkov, AAaKBW. Mitochondrial ROS Production. In: Quek, J., editor. Oxidative Stress, Disease and Cancer. 2005.
13. Kareyeva AV, Grivennikova VG, Vinogradov AD. Mitochondrial hydrogen peroxide production as determined by the pyridine nucleotide pool and its redox state. Biochim Biophys Acta. 2012; 1817(10):1879–1885. [PubMed: 22503830]
14. Korge P, Ping P, Weiss JN. Reactive oxygen species production in energized cardiac mitochondria during hypoxia/reoxygenation: modulation by nitric oxide. Circ Res. 2008; 103(8):873–880. [PubMed: 18776040]
15. Korge P, Honda HM, Weiss JN. Regulation of the mitochondrial permeability transition by matrix Ca(2+) and voltage during anoxia/reoxygenation. Am J Physiol Cell Physiol. 2001; 280(3):C517–C526. [PubMed: 11171571]
16. Gostimskaya IS, Grivennikova VG, Zharova TV, Bakeeva LE, Vinogradov AD. In situ assay of the intramitochondrial enzymes: use of alamethicin for permeabilization of mitochondria. Anal Biochem. 2003; 313(1):46–52. [PubMed: 12576057]
17. Grivennikova VG, Kapustin AN, Vinogradov AD. Catalytic activity of NADH-ubiquinone oxidoreductase (complex I) in intact mitochondria. evidence for the slow active/inactive transition. J Biol Chem. 2001; 276(12):9038–9044. [PubMed: 11124957]
18. Kotlyar AB, Maklashina E, Cecchini G. Absence of NADH channeling in coupled reaction of mitochondrial malate dehydrogenase and complex I in alamethicin-permeabilized rat liver mitochondria. Biochem Biophys Res Commun. 2004; 318(4):987–991. [PubMed: 15147970]
19. Nakagawa S, Cuthill IC. Effect size, confidence interval and statistical significance: a practical guide for biologists. Biol Rev Camb Philos Soc. 2007; 82(4):591–605. [PubMed: 17944619]
20. Efron B, Tibshirani R. Statistical data analysis in the computer age. Science. 1991; 253(5018):390–395. [PubMed: 17746394]
21. Calmettes G, Drummond GB, Vowler SL. Making do with what we have: use your bootstraps. J Physiol. 2012; 590(Pt 15):3403–3406. [PubMed: 22855048]
22. LaNoue KF, Walajtys EI, Williamson JR. Regulation of glutamate metabolism and interactions with the citric acid cycle in rat heart mitochondria. J Biol Chem. 1973; 248(20):7171–7183. [PubMed: 4355202]
23. Borst P. The pathway of glutamate oxidation by mitochondria isolated from different tissues. Biochim Biophys Acta. 1962; 57:256–269. [PubMed: 13871490]
24. Lin RC, Davis EJ. Malic enzymes of rabbit heart mitochondria. Separation and comparison of some characteristics of a nicotinamide adenine dinucleotide-preferring and a nicotinamide adenine dinucleotide phosphate-specific enzyme. J Biol Chem. 1974; 249(12):3867–3875. [PubMed: 4151949]
25. Starkov AA, Fiskum G, Chinopoulos C, Lorenzo BJ, Browne SE, Patel MS, Beal MF. Mitochondrial alpha-ketoglutarate dehydrogenase complex generates reactive oxygen species. J Neurosci. 2004; 24(36):7779–7788. [PubMed: 15356189]

26. Tretter L, Adam-Vizi V. Generation of reactive oxygen species in the reaction catalyzed by alpha-ketoglutarate dehydrogenase. J Neurosci. 2004; 24(36):7771–7778. [PubMed: 15356188]
27. Bunik VI, Denton TT, Xu H, Thompson CM, Cooper AJ, Gibson GE. Phosphonate analogues of alpha-ketoglutarate inhibit the activity of the alpha-ketoglutarate dehydrogenase complex isolated from brain and in cultured cells. Biochemistry. 2005; 44(31):10552–10561. [PubMed: 16060664]
28. Blinova K, Carroll S, Bose S, Smirnov AV, Harvey JJ, Knutson JR, Balaban RS. Distribution of mitochondrial NADH fluorescence lifetimes: steady-state kinetics of matrix NADH interactions. Biochemistry. 2005; 44(7):2585–2594. [PubMed: 15709771]
29. Blinova K, Levine RL, Boja ES, Griffiths GL, Shi ZD, Ruddy B, Balaban RS. Mitochondrial NADH fluorescence is enhanced by complex I binding. Biochemistry. 2008; 47(36):9636–9645. [PubMed: 18702505]
30. McMinn CL, Ottaway JH. Studies on the mechanism and kinetics of the 2-oxoglutarate dehydrogenase system from pig heart. Biochem J. 1977; 161(3):569–581. [PubMed: 192200]
31. Aldakkak M, Stowe DF, Dash RK, Camara AK. Mitochondrial handling of excess Ca2+ is substrate-dependent with implications for reactive oxygen species generation. Free Radic Biol Med. 2013; 56:193–203. [PubMed: 23010495]
32. Chen Q, Vazquez EJ, Moghaddas S, Hoppel CL, Lesnefsky EJ. Production of reactive oxygen species by mitochondria: central role of complex III. J Biol Chem. 2003; 278(38):36027–36031. [PubMed: 12840017]
33. Dugan LL, You YH, Ali SS, Diamond-Stanic M, Miyamoto S, DeCleves AE, Andreyev A, Quach T, Ly S, Shekhtman G, Nguyen W, Chepetan A, Le TP, Wang L, Xu M, Paik KP, Fogo A, Viollet B, Murphy A, Brosius F, Naviaux RK, Sharma K. AMPK dysregulation promotes diabetes-related reduction of superoxide and mitochondrial function. J Clin Invest. 2013; 123(11):4888–4899. [PubMed: 24135141]
34. Gyulkhandanyan AV, Pennefather PS. Shift in the localization of sites of hydrogen peroxide production in brain mitochondria by mitochondrial stress. J Neurochem. 2004; 90(2):405–421. [PubMed: 15228597]
35. Heinen A, Aldakkak M, Stowe DF, Rhodes SS, Riess ML, Varadarajan SG, Camara AK. Reverse electron flow-induced ROS production is attenuated by activation of mitochondrial Ca2+-sensitive K+ channels. Am J Physiol Heart Circ Physiol. 2007; 293(3):H1400–H1407. [PubMed: 17513497]
36. Hoegger MJ, Lieven CJ, Levin LA. Differential production of superoxide by neuronal mitochondria. BMC Neurosci. 2008; 9:4. [PubMed: 18182110]
37. Ohnishi ST, Ohnishi T, Muranaka S, Fujita H, Kimura H, Uemura K, Yoshida K, Utsumi K. A possible site of superoxide generation in the complex I segment of rat heart mitochondria. J Bioenerg Biomembr. 2005; 37(1):1–15. [PubMed: 15906144]
38. Batandier C, Leverve X, Fontaine E. Opening of the mitochondrial permeability transition pore induces reactive oxygen species production at the level of the respiratory chain complex I. J Biol Chem. 2004; 279(17):17197–17204. [PubMed: 14963044]
39. Johansson FI, Michalecka AM, Moller IM, Rasmusson AG. Oxidation and reduction of pyridine nucleotides in alamethicin-permeabilized plant mitochondria. Biochem J. 2004; 380(Pt 1):193–202. [PubMed: 14972026]
40. Matic S, Geisler DA, Moller IM, Widell S, Rasmusson AG. Alamethicin permeabilizes the plasma membrane and mitochondria but not the tonoplast in tobacco (Nicotiana tabacum L. cv Bright Yellow) suspension cells. Biochem J. 2005; 389(Pt 3):695–704. [PubMed: 15836437]
41. Shore JD, Evans SA, Holbrook JJ, Parker DM. NADH binding to porcine mitochondrial malate dehydrogenase. J Biol Chem. 1979; 254(18):9059–9062. [PubMed: 225321]
42. Sumegi B, Srere PA. Complex I binds several mitochondrial NAD-coupled dehydrogenases. J Biol Chem. 1984; 259(24):15040–15045. [PubMed: 6439716]
43. Ovadi J, Huang Y, Spivey HO. Binding of malate dehydrogenase and NADH channelling to complex I. J Mol Recognit. 1994; 7(4):265–272. [PubMed: 7734152]
44. Amarneh B, Vik SB. Direct transfer of NADH from malate dehydrogenase to complex I in Escherichia coli. Cell Biochem Biophys. 2005; 42(3):251–261. [PubMed: 15976458]

45. Fahien LA, Teller JK. Glutamate-malate metabolism in liver mitochondria. A model constructed on the basis of mitochondrial levels of enzymes, specificity, dissociation constants, and stoichiometry of hetero-enzyme complexes. J Biol Chem. 1992; 267(15):10411–10422. [PubMed: 1350279]
46. Fahien LA, Kmiotek EH, MacDonald MJ, Fibich B, Mandic M. Regulation of malate dehydrogenase activity by glutamate, citrate, alpha-ketoglutarate, and multienzyme interaction. J Biol Chem. 1988; 263(22):10687–10697. [PubMed: 2899080]
47. Fahien LA, MacDonald MJ, Teller JK, Fibich B, Fahien CM. Kinetic advantages of hetero-enzyme complexes with glutamate dehydrogenase and the alpha-ketoglutarate dehydrogenase complex. J Biol Chem. 1989; 264(21):12303–12312. [PubMed: 2745445]
48. Kay L, Nicolay K, Wieringa B, Saks V, Wallimann T. Direct evidence for the control of mitochondrial respiration by mitochondrial creatine kinase in oxidative muscle cells in situ. J Biol Chem. 2000; 275(10):6937–6944. [PubMed: 10702255]
49. Saks V, Beraud N, Wallimann T. Metabolic compartmentation - a system level property of muscle cells: real problems of diffusion in living cells. Int J Mol Sci. 2008; 9(5):751–767. [PubMed: 19325782]
50. Mullinax TR, Mock JN, McEvily AJ, Harrison JH. Regulation of mitochondrial malate dehydrogenase. Evidence for an allosteric citrate-binding site. J Biol Chem. 1982; 257(22):13233–13239. [PubMed: 7142142]
51. Bellamy D. The endogenous citric acid cycle intermediates and amino acids of mitochondria. Biochemical Journal. 1961; 82:218–224. [PubMed: 13866863]
52. Olson MSVKR. Changes in endogenous substrates of isolated rabbit heart mitochondria during storage. J Biol Chem. 1967; 242(2):325–332. [PubMed: 6016618]
53. Murphy E, Coll KE, Viale RO, Tischler ME, Williamson JR. Kinetics and regulation of the glutamate-aspartate translocator in rat liver mitochondria. J Biol Chem. 1979; 254(17):8369–8376. [PubMed: 38250]
54. Drose S, Brandt U. The mechanism of mitochondrial superoxide production by the cytochrome bc1 complex. J Biol Chem. 2008; 283(31):21649–21654. [PubMed: 18522938]
55. Drose S, Bleier L, Brandt U. A common mechanism links differently acting complex II inhibitors to cardioprotection: modulation of mitochondrial reactive oxygen species production. Mol Pharmacol. 2011; 79(5):814–822. [PubMed: 21278232]
56. Quinlan CL, Gerencser AA, Treberg JR, Brand MD. The mechanism of superoxide production by the antimycin-inhibited mitochondrial Q-cycle. J Biol Chem. 2011; 286(36):31361–31372. [PubMed: 21708945]
57. Dennis SC, Clark JB. The regulation of glutamate metabolism by tricarboxylic acid-cycle activity in rat brain mitochondria. Biochem J. 1978; 172(1):155–162. [PubMed: 656069]
58. Gardner PR. Aconitase: sensitive target and measure of superoxide. Methods Enzymol. 2002; 349:9–23. [PubMed: 11912933]
59. Tretter L, Adam-Vizi V. Inhibition of Krebs cycle enzymes by hydrogen peroxide: A key role of [alpha]-ketoglutarate dehydrogenase in limiting NADH production under oxidative stress. J Neurosci. 2000; 20(24):8972–8979. [PubMed: 11124972]
60. Chinopoulos C. Which way does the citric acid cycle turn during hypoxia? The critical role of alpha-ketoglutarate dehydrogenase complex. J Neurosci Res. 2013; 91(8):1030–1043. [PubMed: 23378250]
61. Leyssens A, Nowicky AV, Patterson L, Crompton M, Duchen MR. The relationship between mitochondrial state, ATP hydrolysis, (Mg-2+)-i and (Ca-2+)-i studied in isolated rat cardiomyocytes. Journal of Physiology (Cambridge). 1996; 496(1):111–128.

Highlights

- We studied malate/glutamate-stimulated ROS production after complex I inhibition
- Permeabilization revealed substrate/enzyme interactions essential for ROS production
- ROS generation depends on local NADH production to generate a high $NADH/NAD^+$ ratio
- A high $NADH/NAD^+$ ratio requires functional coupling between MDH and AST
- Oxaloacetate removal and CoA-dependent ketoglutarate oxidation play key roles

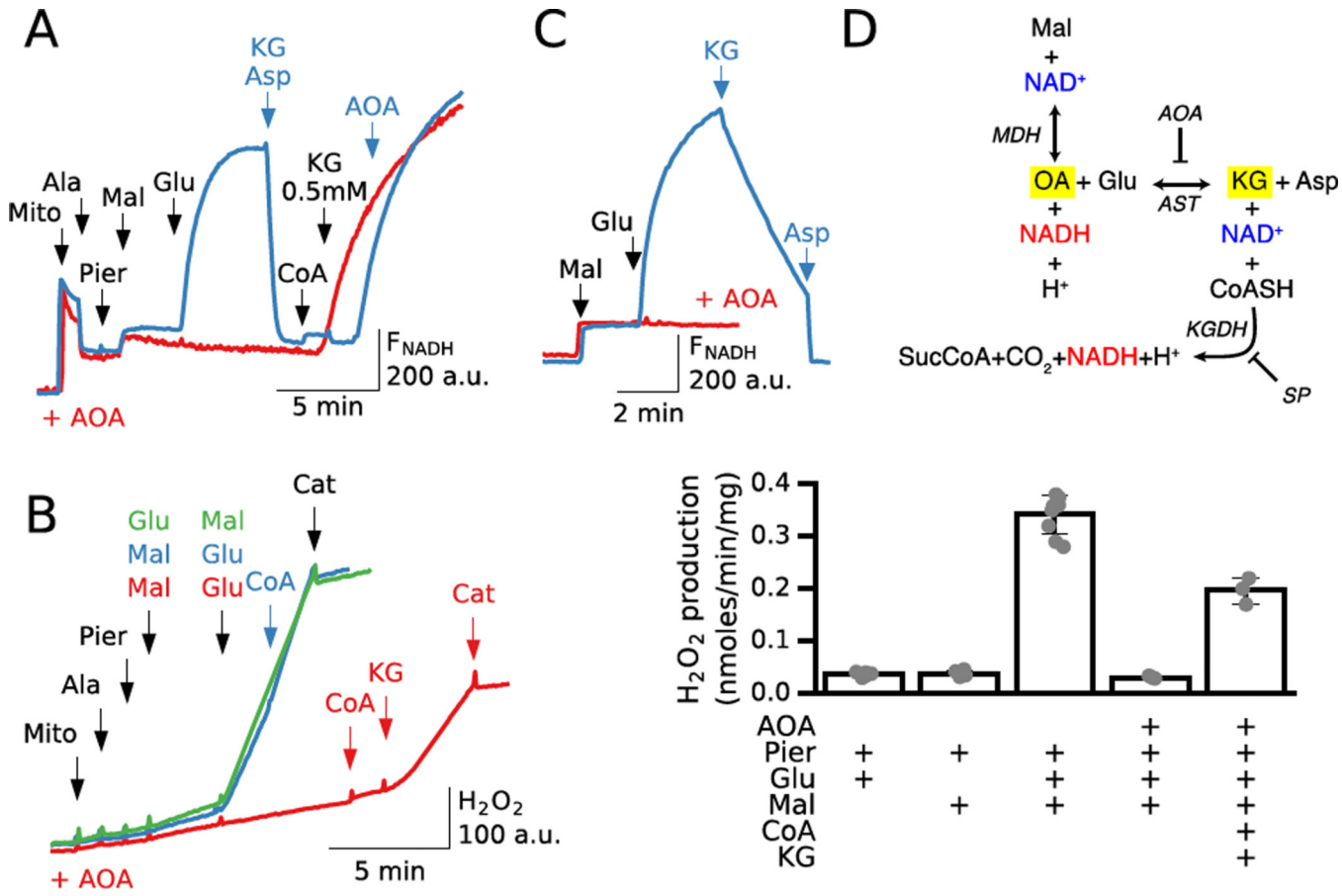

Fig. 1. Malate/glutamate-induced NADH and ROS production depends on functional coupling between malate dehydrogenase (MDH) and aspartate aminotransaminase (AST)

Additions to all traces are indicated by black arrows; additions to one trace only are indicated by the same color arrows. **A.** Mitochondria incubated with NAD^+ (200 μM) in the absence (blue trace) or presence of the AST inhibitor AOA (0.5 mM) (red trace) were permeabilized with alamethicin (Ala) and inhibited with piericidin (Pier, 0.2 μM) before adding malate (Mal) and then glutamate (Glu) (both 5 mM). In the absence of AOA (blue trace), NAD(P)H fluorescence ($F_{NAD(P)H}$) did not increase signficantly with malate alone until glutamate was also added. Addition of α-ketoglutarate (KG) and aspartate (Asp) (0.25 mM each) to reverse the coupled MDH/AST reactions resulted in rapid oxidation of NADH. Adding CoA (0.2 mM) and KG (0.5 mM) had no significant effect until AOA was added to prevent NADH oxidation by MDH and allow NADH generation by α-ketoglutarate dehydrogenase (KGDH). In contrast, pretreatment with AOA (0.5 mM, red trace) prevented the malate/glutamate-induced increase in NADH until CoA and KG were added to stimulate NADH generation by KGDH. **B**. Corresponding H_2O_2 production by permeabilized mitochondria under similar conditions used to measure NADH production in A, with either 5 mM malate (blue trace) or 5 mM glutamate (green trace) added before the other substrate. Malate and glutamate alone had no effect on H_2O_2 production, but the combination increased H_2O_2 production, which was not further enhanced by CoA (0.2 mM). If mitochondria were incubated with AOA (0.5 mM) before adding substrates (red trace), H_2O_2 production by malate/glutamate was suppressed. Under these conditions, addition of

CoA (0.2 mM) and KG (0.5 mM) to activate ROS production by KGDH increased H_2O_2 production, but to a lesser extent. At the end of all the traces, catalase (Cat, 2 μM) was added to show that increase in fluorescence was due to H_2O_2 production. **Bar graph** shows average H2O2 production for 3–5 preparations under those different conditions. **C.** Demonstration that AST and glutamate are required to enhance NADH production by MDH. Purified MDH (22 μg) and AST (15 μg) were incubated with NAD^+ (100 μM) in the absence or presence of 0.25 mM AOA. Addition of 2 mM malate caused a rapid but small increase in NADH fluorescence, consistent with rapid product inhibition by oxaloacetate and NADH accumulation. In the absence of AOA (blue trace), addition of glutamate (2 mM) rapidly increased NADH generation, which was reversed by adding KG and aspartate (10 mM each). In presence of AOA (red trace), the effect of glutamate on NADH generation was completely prevented. **D**. Schema of the MDH, AST and KGDH reactions. SP is succinyl phosphonate, a potent inhibitor of KGDH.

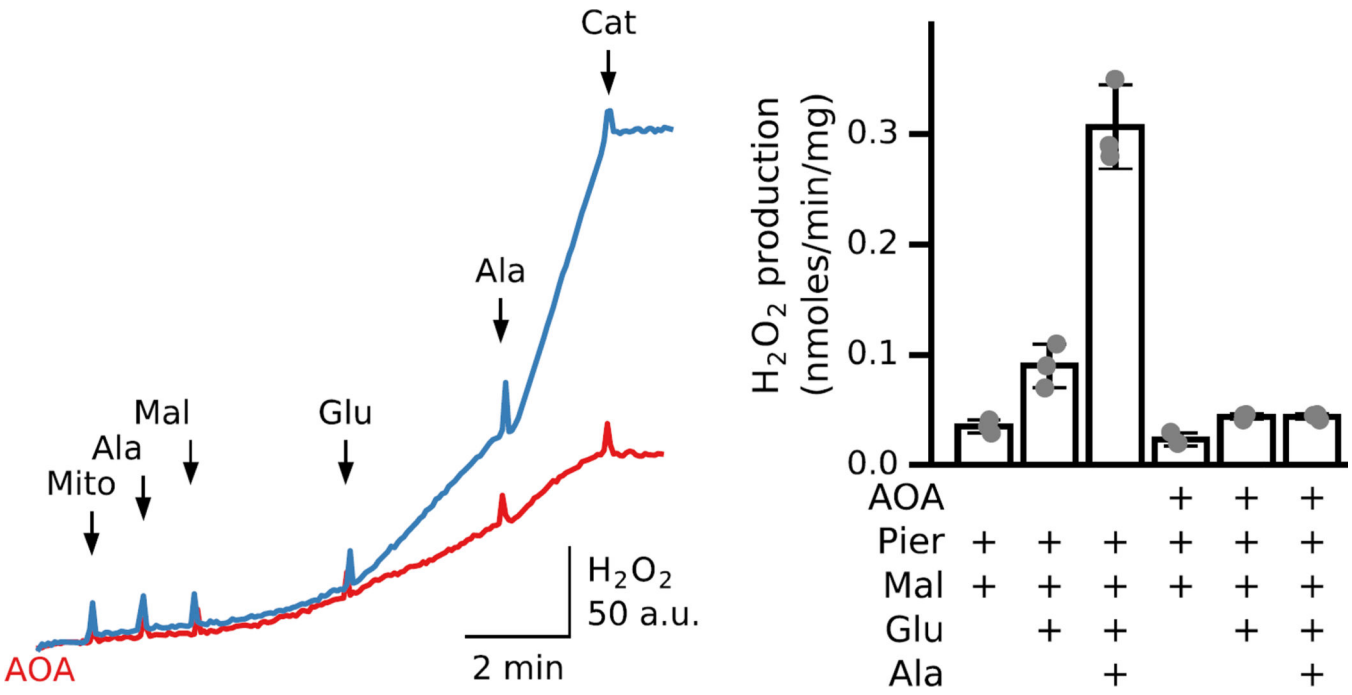

Fig. 2. Malate/glutamate-induced ROS production in intact, piericidin-inhibited mitochondria

Mitochondria incubated in the presence (red trace) or absence (blue trace) of AOA (1mM) to inhibit AST were inhibited with piericidin (0.5 μM). Malate and glutamate (5 mM each) were added as indicated, followed by alamethicin and catalase. **Bar graph** shows average H_2O_2 production for 3 preparations under those different conditions

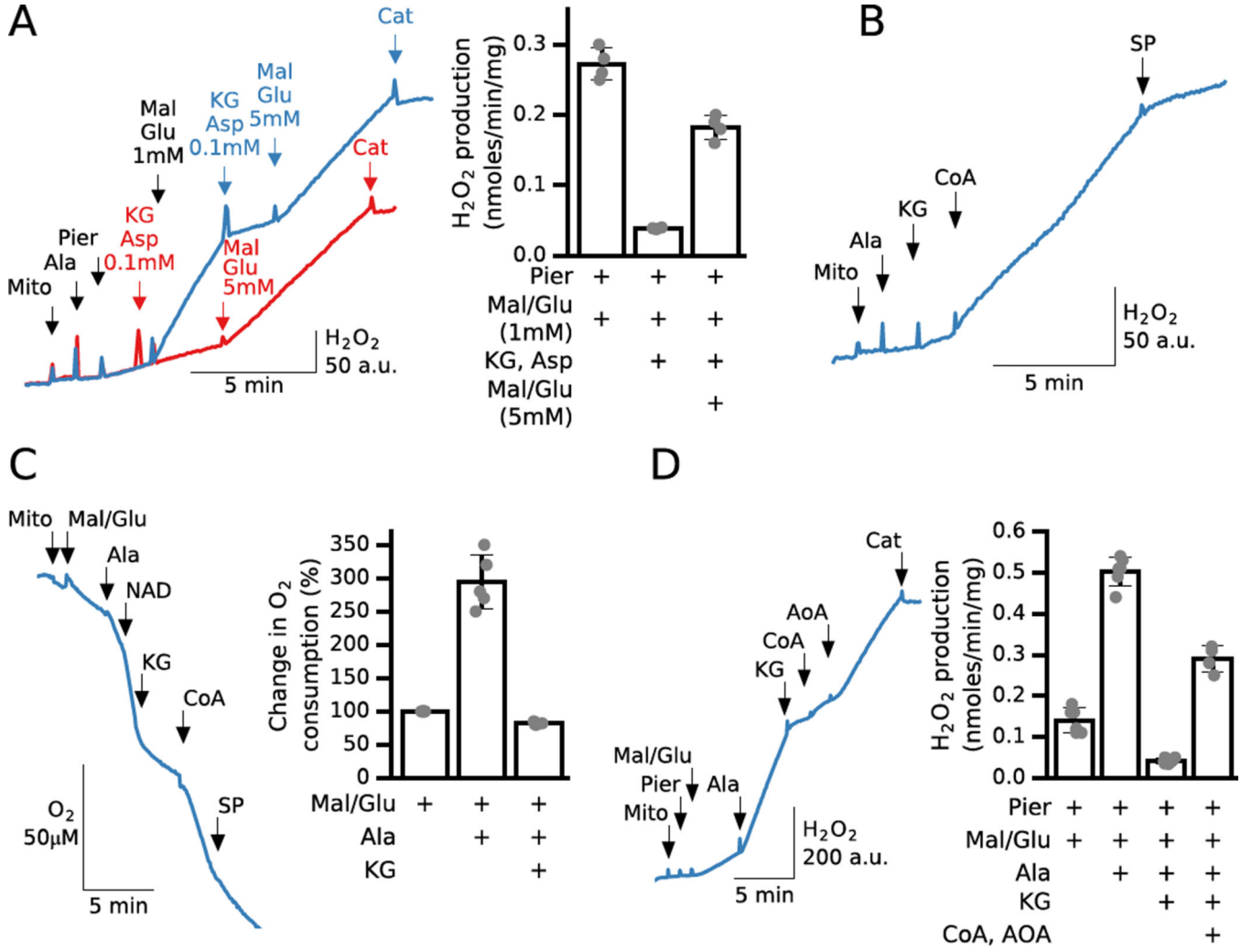

Fig. 3. A. Reversal of MDH/AST reactions with α-ketoglutarate (KG) and aspartate (Asp) inhibits malate/glutamate-induced H_2O_2 production

Additions to all traces are indicated by black arrows; additions to one trace only are indicated by the same color arrows. In permeabilized mitochondria inhibited by piericidin (Pier, 200 nM), H_2O_2 production increased after adding malate (Mal) and glutamate (Glu) (1 mM each) and then was rapidly inhibited by KG and Asp (0.1 mM each) (blue trace). Addition of KG and Asp before malate/glutamate (1 mM) prevented the increase in H_2O_2 production (red trace). In both cases, additional malate/glutamate (5 mM each) to change the MDH/AST equilibrium in favor of NADH production stimulated H_2O_2 production. **Bar graph** shows average H2O2 production for 4 preparations under those different conditions. **B. H_2O_2 production by KGDH during KG oxidation requires CoA addition in permeabilized mitochondria**. After permeabilization, addition of KG (2 mM) and CoA (0.3 mM) stimulated H_2O_2 production (0.1 nmol/min/mg), which was suppressed by adding the KGDH inhibitor succinyl phosphonate (SP, 2mM). **C. Alamethicin addition to malate/glutamate (5 mM each) energized mitochondria accelerated O_2 consumption** that was rapidly inhibited with KG (2 mM), further activated with CoA (0.2 mM) and inhibited with SP (1 mM) addition. **Bar graph** shows relative change in O2 consumption after alamethicin

and KG addition. Malate/glutamate stimulate O2 consumption before alamethicin is taken for 100%. **D. Alamethicin addition during malate/glutamate-stimulated ROS production by piericidin-inhibited (0.2 μM) intact mitochondria** significantly accelerated ROS generation that was inhibited with KG (2 mM) and activated by AOA (0.5 mM) after CoA addition. **Bar graph** shows average H2O2 production for 4–6 preparations under those different conditions.

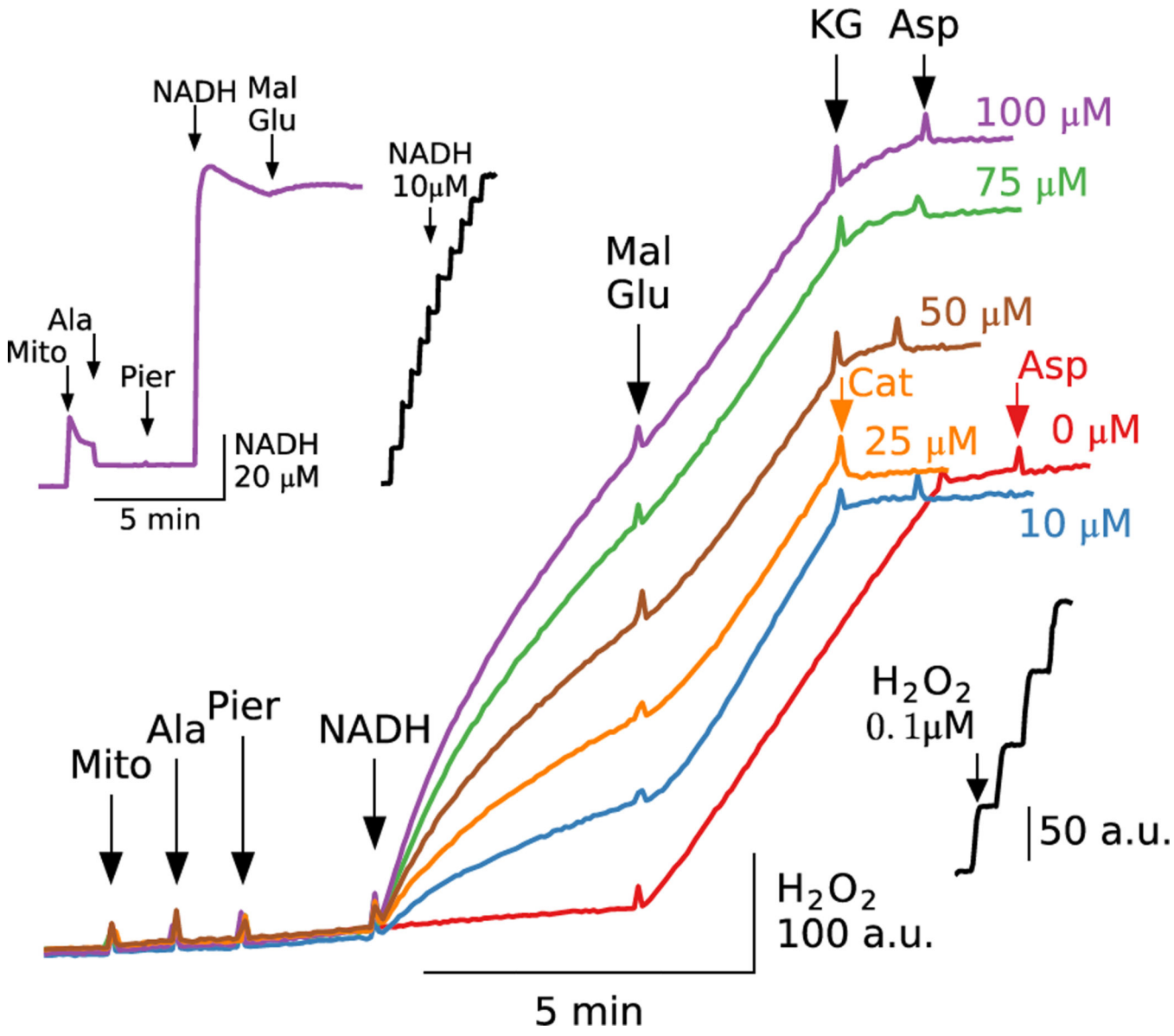

Fig. 4. NADH-induced ROS production in piericidin-inhibited permeabilized mitochondria depends on the matrix NADH/NAD$^+$ ratio rather than total [NADH]

Additions to all traces are indicated by black arrows; additions to one trace only are indicated by the same color arrows. Piericidin (Pier, 500 nM) was added to permeabilized mitochondria followed by NADH at the concentrations indicated at the end of the trace. Addition of malate (Mal) and glutamate (Glu) (5 mM each) accelerated H_2O_2 production to similar levels in all cases, despite the different amounts of NADH added. Adding α-ketoglutarate (KG) and aspartate (Asp) (5 mM each), or catalase (Cat), suppressed H_2O_2 production. **Inset** in left upper corner shows changes in NADH fluorescence after 100 μM NADH was added to piericidin-inhibited permeabilized mitochondria. After reaching a peak, NADH fluorescence declined slowly, but then increased with addition of malate and glutamate, consistent with the maintained H_2O_2 production in the main panel (purple trace).

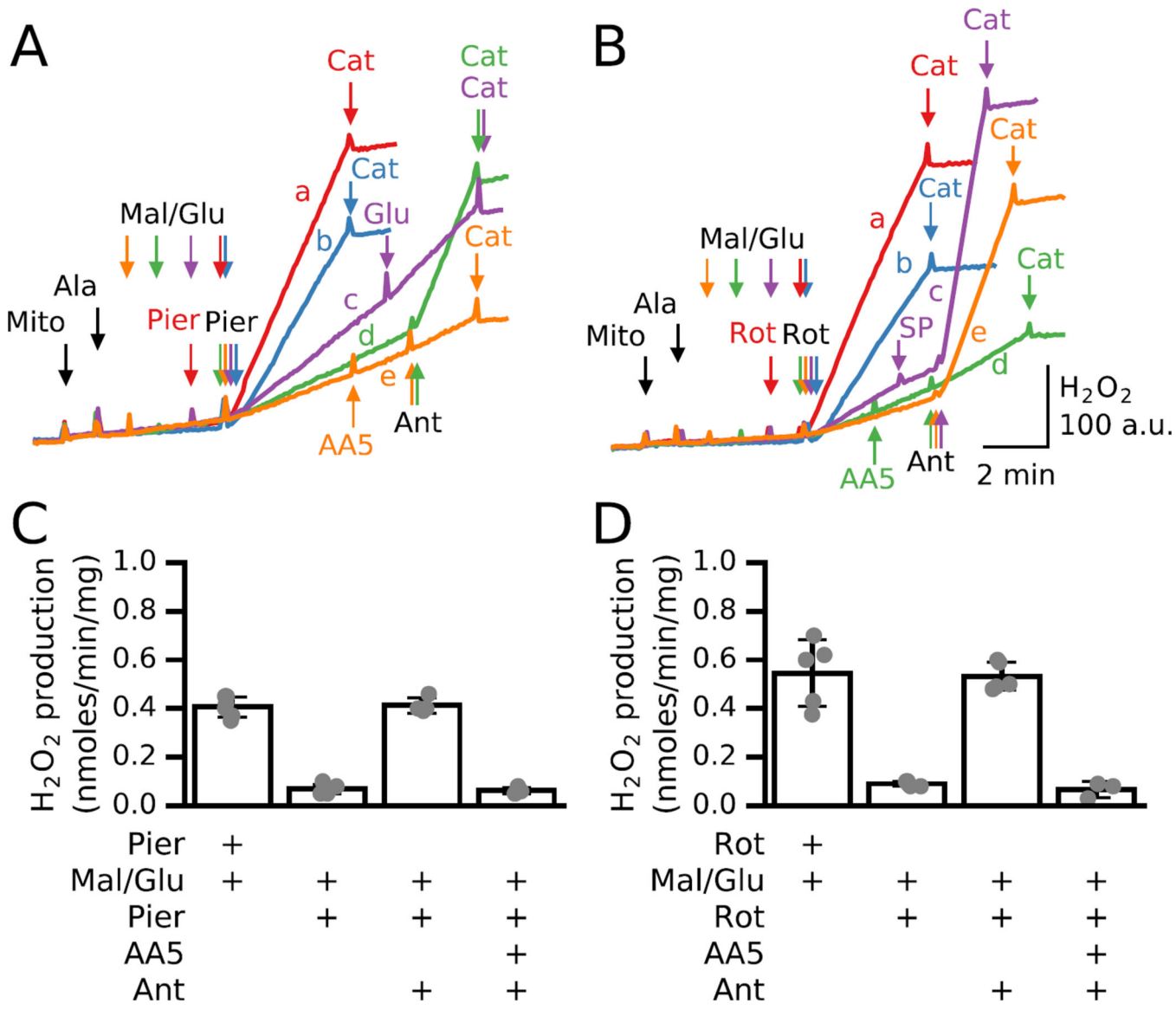

Fig. 5. H_2O_2 production by permeabilized mitochondria depends on whether piericidin or rotenone are added before or after malate/glutamate

Additions to all traces are indicated by black arrows; additions to one trace only are indicated by the same color arrows. **A.** H_2O_2 production when piericidin (Pier, 200 nM) was added before malate (Mal) and glutamate (Glu) (5 mM each) was 0.45 nmol/min/mg and terminated by catalase (Cat) (red trace a). In the same preparation, H_2O_2 production was progressively reduced when piericidin was added immediately (blue trace b), 1 min (purple trace c), 2 min (green trace d) or 3 min (orange trace e) after malate /glutamate. In trace c 10 mM glutamate (10 mM) and in traces d and e, antimycin (Ant, 1 μM) was also added. In trace e, the complex II inhibitor atpenin A5 (AA5, 250 nM) was added before antimycin. **B**. Same as A, but with rotenone (2 μM) in place of piericidin. In trace c, antimycin was added after inhibition of KG oxidation by KGDH with SP (1.5 mM). In traces d and e, antimycin was added. In trace d atpenin (AA5 250 nM) was added before antimycin. **C,D**. Average H_2O_2 production (nmoles/min/mg) in 4–6 preparations of permeabilized mitochondria

inhibited with 200 nM piericidin (**C**) or 2 μM rotenone (**D**) added before or 2 min after malate/glutamate (5 mM each). In the latter case, H_2O_2 production after adding antimycin in the absence or presence of complex II inhibitor AA5 is also shown.

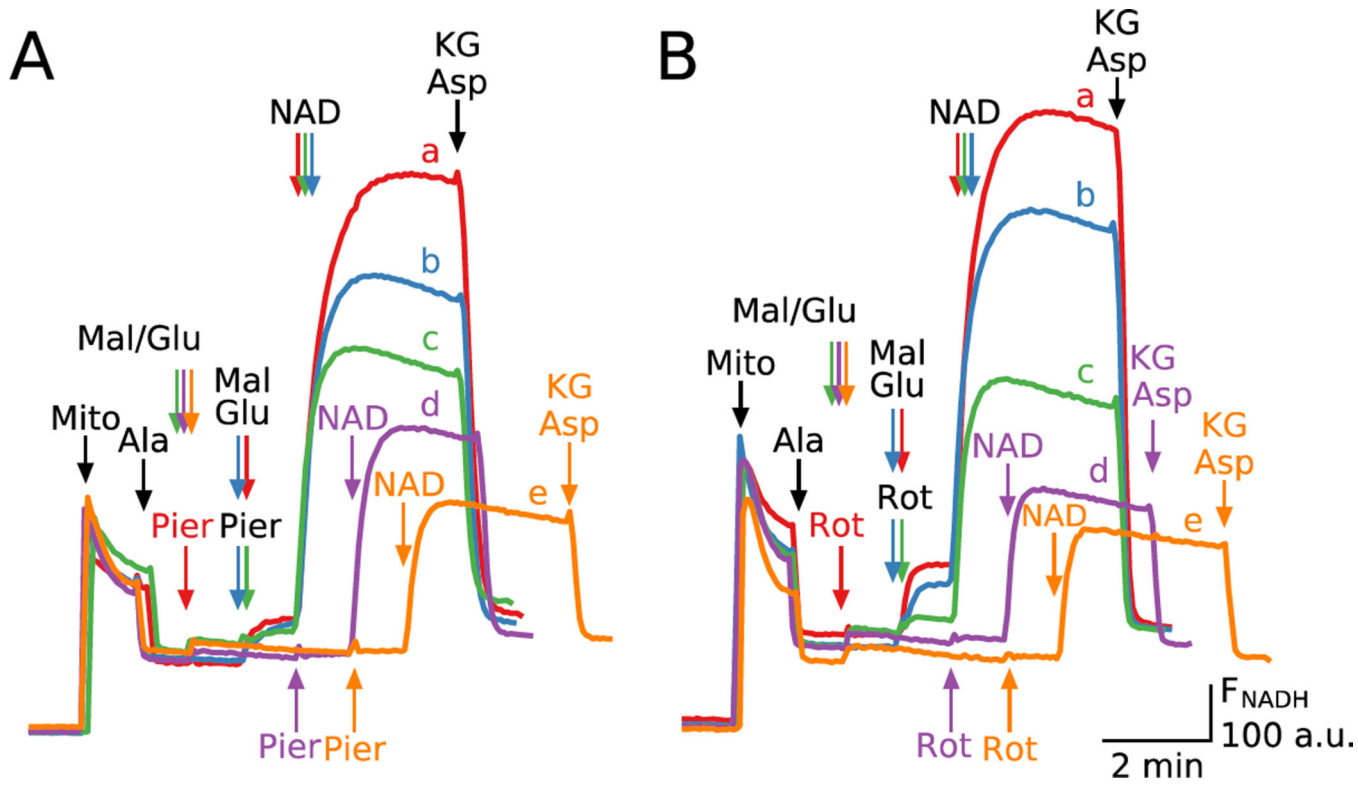

Fig. 6. NADH production by permeabilized mitochondria depends on whether piericidin or rotenone are added before or after malate/glutamate

Additions to all traces are indicated by black arrows; additions to one trace only are indicated by the same color arrows. **A.** NADH production after adding exogenous NAD^+ (200 μM) when piericidin (Pier, 200 nM) was added before malate (Mal) and glutamate (Glu) (5 mM), followed by α-ketoglutarate (KG) and aspartate (Asp) (0.25 mM each) (red trace a). Same preparation, but with piericidin added immediately (blue trace b), 1 min (green trace c), 2 min (purple trace d) or 3 min (orange trace e) after malate and glutamate. **B**. Same as **A**, but with rotenone (2 μM) in place of piericidin

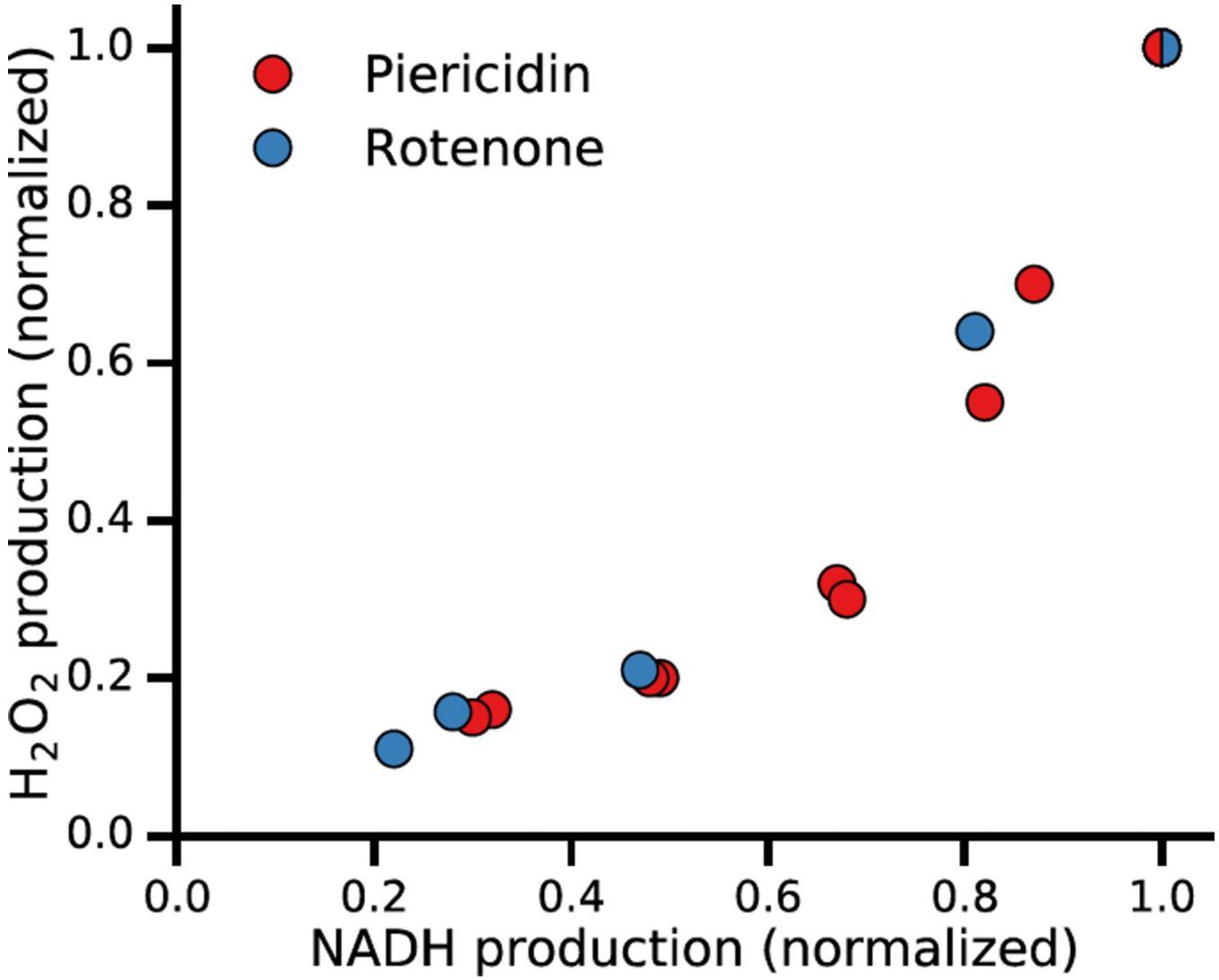

Fig. 7.

The relationship between NADH and H_2O_2 production (for the data shown in Figs. 5 and 6).

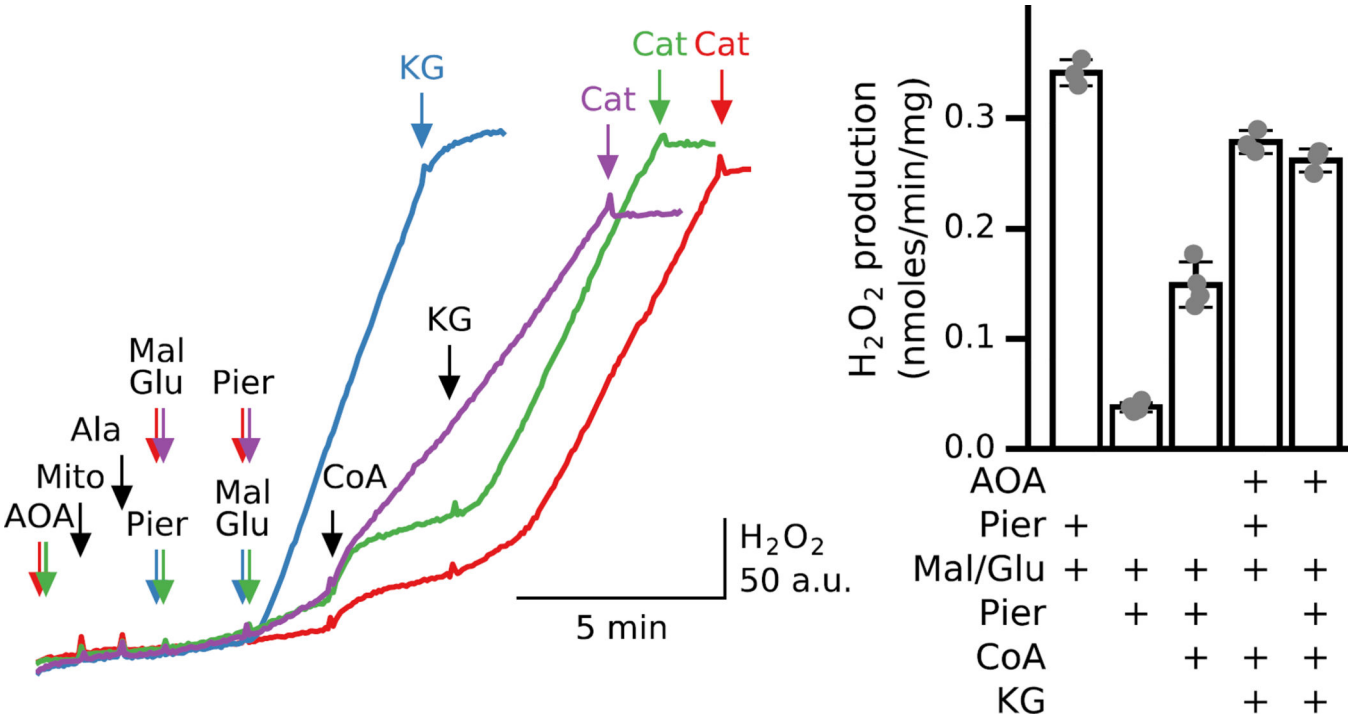

Fig. 8. CoA increases H_2O_2 production in permeabilized mitochondria exposed to malate/glutamate before piericidin

Additions to all traces are indicated by black arrows; additions to one trace only are indicated by the same color arrows. Compared to when piericidin (Pier, 200 nM) was added before malate (Mal) and glutamate (Glu) (5 mM each, blue trace), piericidin added to permeabilized mitochondria 2 min after malate/glutamate had very little effect on H_2O_2 production (purple trace) as in Fig. 5A. However, addition of CoA (0.2 mM) significantly accelerated H_2O_2 production. In the presence of AOA (1mM) CoA effect was absent, but further addition of KG (5 mM) significantly increased H2O2 production irrespective whether piericidin was added before (green trace) or after (red trace) substrates. **Bar graph** Shows average H2O2 production for 3–4 preparations under those different conditions.

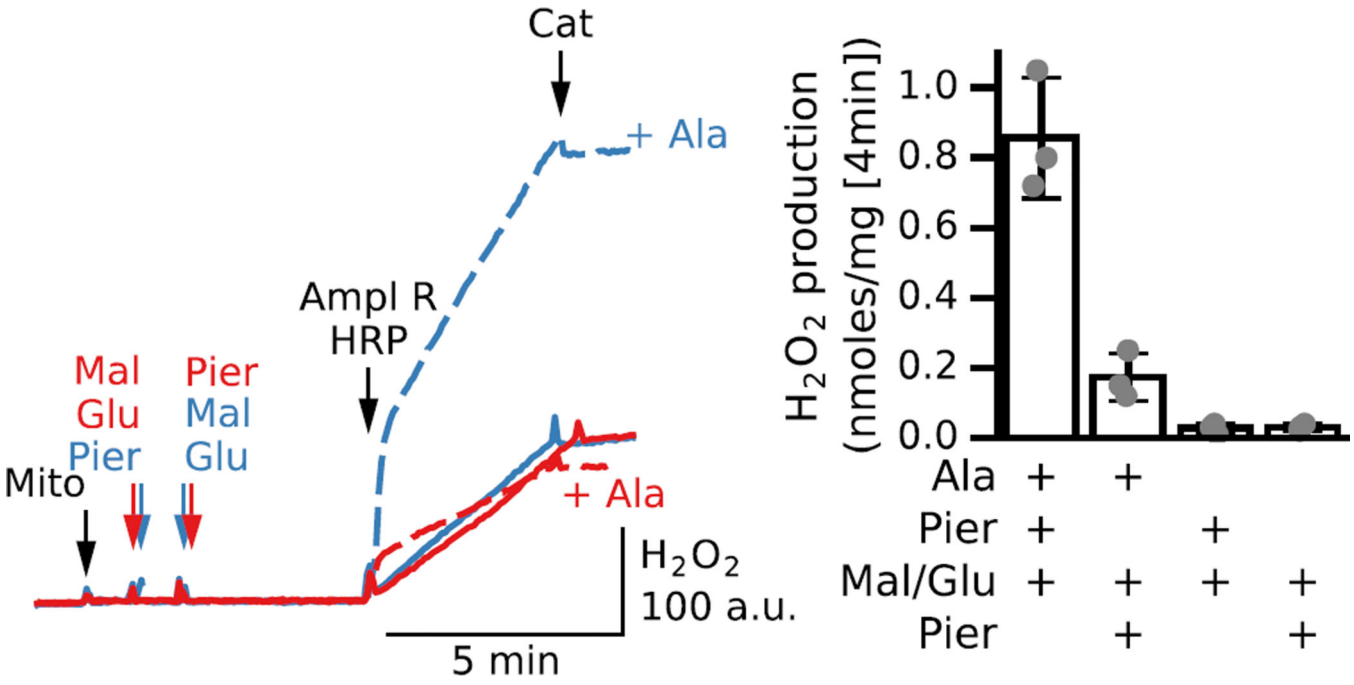

Fig. 9. Permeabilization reveals differences in piericidin-induced H_2O_2 production by decreasing mitochondrial H_2O_2 scavenging power

Additions to all traces are indicated by black arrows; additions to one trace only are indicated by the same color arrows. Mitochondria were incubated in the absence or presence of alamethicin (+Ala). Complex I was inhibited by piericidin (Pier, 150 nM) before (blue trace) or after (red trace) malate (Mal) and glutamate (Glu) (5 mM each) in either intact (solid lines) or permeabilized mitochondria (dashed lines). Amplex Red/HRP were added after 4 min incubation, showing that H_2O_2 had accumulated in the buffer in permeabilized mitochondria but not in intact mitochondria, as indicated by the sudden jump in Amplex Red/HRP fluorescence. **Bar graph** shows average increase in [H2O2] after Amplex red/HRP addition for 3 preparations of intact or permeabilized mitochondria incubated with piericidin and malate/glutamate added before or after inhibitor.